

Experimental study of convective heat transfer coefficient of MgO nanofluid in a cylindrical microchannel heat sink

Omid Torabipour, Zoha Azizi*

Department of Chemical Engineering, Mahshahr branch, Islamic Azad University, Mahshahr, Iran

Received 8 February 2018;

revised 18 March 2018;

accepted 21 April 2018;

available online 6 May 2018

ABSTRACT: Convective heat transfer of MgO-water nanofluid in a microchannel heat sink is experimentally investigated in various concentrations of 0.01, 0.05, 0.1, and 0.6 wt%. The microchannel consisted of 48 parallel rectangular cross section channels with the height of 800 μm , width of 524 μm and length of 52 mm. A well stability duration (ca. 1 month) was resulted by a 180 min ultrasonication of the MgO suspension. The experiments in the microchannel were then performed in a flow rate range of 0.5 to 2.2 l/min while the inlet temperature and heat flux were constant. The results indicated that using the MgO nanofluid in low flow rates and concentration has less effect in improving the heat transfer coefficient, while it becomes highly efficient by the simultaneous increase of flow rate and concentration. An enhancement of 162.3% in convective heat transfer coefficient at the channel inlet was achieved at the concentration of 0.6 wt% and the flow rate of 2.2 l/min, and at the same condition, the average Nusselt number also increased up to 52.8%. However, the nanofluid at 0.1 wt% was more efficient compared to the other concentrations in increasing Nu at higher Re.

KEYWORDS: Convective heat transfer coefficient; Microchannel heat sink; MgO nanofluid; Stability

INTRODUCTION

As today's electronic devices have become compact, the modern techniques of cooling are substituted for the conventional ones. The heat sinks and heat exchangers are benefited from the developments achieved in electronics and material science, which makes it possible to construct such devices in miniature. Microchannel heat sinks, are a new class of heat sinks first proposed by Tuckerman and Pease [1]. They revealed to be very efficient and suitable for high heat removal from small surfaces. The channel hydraulic diameter is usually less than 1 mm, and this microscopic size reduces and thins the thermal boundary layer, which reduces thermal resistance and, consequently, increases the amount of heat transfer [2, 3]. In the issue of heat transfer efficiency in equipment such as heat exchangers, thermal conductivity of the working fluid plays a major role [4]. Common fluids in heat transfer used in industries are usually fluids such as water, oils, and ethylene glycol. With increasing global competition in various industries and the role of energy in production costs, these industries are increasingly moving towards the development of advanced and new fluids with high thermal performance. Nanofluids increase thermophysical properties (thermal conductivity, thermal diffusivity, viscosity and convective heat transfer coefficient) in comparison with base fluids such as water or oil [5-8]. Due to the ability of the nanoparticles in increasing the heat transfer,

the necessary size of heat exchangers will be smaller [7].

Several studies have been carried out on microchannels, and in particular the use of nanofluids as the working fluid in this device, but the results have been contradictory, and the amount of laboratory research in this area is still low. Reembolet et al. [9] conducted a laboratory research on the hydraulic and thermal properties of copper nanofluid in a rectangular cross-section microwave channel. They used various concentrations of 0.24, 1.03 and 4.5 vol%.

The transient of regime from laminar to turbulent occurred in the critical Reynolds number of 1000. Their results showed a significant increase in heat transfer at the concentrations of 0.24 and 0.3% vol. Peyghambarzadeh et al. [10] experimentally studied the heat transfer of water and water based nanofluids of copper oxide and alumina separately, in a microchannel heat sink. The results showed that nanofluid of copper oxide at a volume fraction of 0.02% and alumina at 1% increased the heat transfer coefficients up to 27 and 49%, respectively. Previously, a cylindrical microchannel was proposed in which the effect of copper-water nanofluid on heat transfer coefficients was investigated by Azizi et al. [11, 12]. The concentrations of nanofluids were 0.05, 0.1 and 0.3 wt%, for which the increase in Nusselt number was reported to be 17, 19 and 23% respectively. In this paper, a water-based MgO nanofluid is used as a cooling fluid in a cylindrical microchannel.

*Corresponding Author Email: azizi.zoha@gmail.com
Tel.: +989112530678; Note. This manuscript was submitted on February 8, 2018; approved on March 18, 2018; published online May 6, 2018.

Nomenclature		Greek Symbols	
cp	Heat capacity, $\text{Jkg}^{-1} \text{K}^{-1}$	ρ	Density, kgm^{-3}
Dh	Hydraulic diameter, m	η	fin efficiency
h	Heat transfer coefficient, $\text{Wm}^{-2}\text{K}^{-1}$	μ	Viscosity, $\text{kg m}^{-1} \text{s}^{-1}$
Hch	Height of channel, m	Φ	volume fraction
k	Thermal conductivity, $\text{Wm}^{-1}\text{K}^{-1}$	Subscripts	
L	Length of channel, m	b	bulk
m	Mass flow rate, kgs^{-1}	bf	base fluid
N	Number of channels	conv	convection
Nu	Nusselt number	in	inlet
q_f	Heat power, W	nf	nanofluid
q''	Heat flux, Wm^{-2}	out	outlet
Re	Reynolds number, $(\rho u)Dh/(\mu)$	p	particle
s	Distance between the thermocouple and the wall, m	s	substrate
T	Temperature, K	th	thermocouple
u_m	Velocity, ms^{-1}	w	wall
W_{ch}	Width of channel, m	z	local
Z	Axiak distance from inlet, m		

It was aimed to study the effect of varied concentrations, hence the nanofluids were prepared at four concentrations of 0.01%, 0.05%, 0.1 % and 0.6%, which are the regular concentrations of various nanofluids used in heat transfer works [11-16]. The effect of nanofluid concentration at different Reynolds number on the forced convective heat transfer coefficient was investigated and the results were compared with the conventional heat transfer relations. The inlet temperature was constant and the flow regime was laminar. The experimental results of the heat transfer coefficient of the nanofluid were compared with the results of using pure water as a cooling fluid.

EXPERIMENTAL

Nanofluid stability

To prepare a magnesium oxide -water nanofluid, the nanoparticles at a specific value were dispersed in pure water. The pack of nanoparticles was purchased from Us Research Nanomaterial Inc. and its specifications are reported in Table 1 accompanied by its TEM image presented in Figure 1.

Table 1
The specifications of MgO nanoparticles.

Nano particle size (nm)	Purity	True density (g/cm^3)	Bulk density (g/cm^3)	Color	Specific heat (J/kg.K)	Thermal conductivity (W/m.K)
20	98%	3.58	0.145	white	985	56

The suspension at the desired concentration was prepared in a volume of 1.5 liters using a sonication bath for 180 minutes. Then, the stability of the suspension was monitored in static condition for thirty days. No sediments were observable during this period of time which indicates

that a stable nanofluid is prepared which is suitable for cooling purposes.

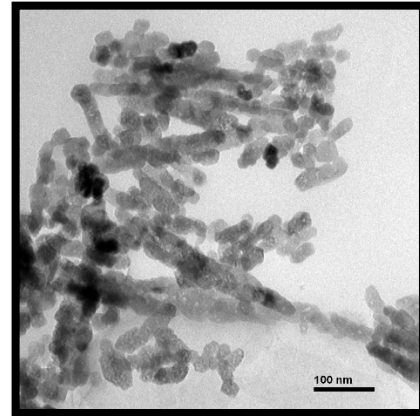


Fig. 1. TEM image of the MgO nanoparticles

Microchannel heat sink

The main part of the prepared laboratory system is the microchannel alloy, which is made of copper metal. On the surface, 48 rectangular cross section micro-channels were created by a Wire Cut machine the method of which is explained elsewhere [11].

The width of each channel is $524 \mu\text{m}$ and its height is $800 \mu\text{m}$ and has a $632 \mu\text{m}$ hydraulic diameter. This module has an internal diameter of 2 cm and a height of 52 mm. A picture of the modulus used in this study is depicted in Figure 2.

To measure the temperature along the microchannel wall, four thermocouples were inserted at the same radius but at different axial distances.

The position of these thermocouples in the module is presented in Table 2.

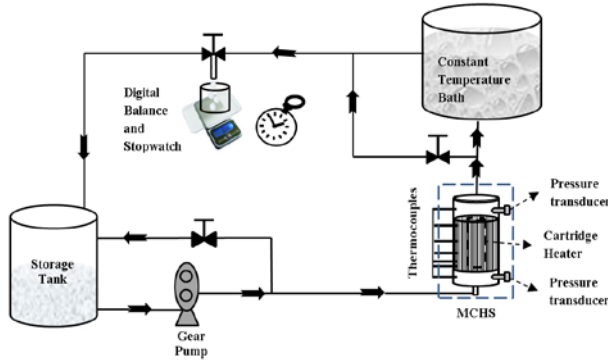
Table 2

Positions of the thermocouples inside the microchannel.

Thermocouple label	T1	T2	T3	T4
Axial distance from inlet (mm)	3	10	32	44


Fig. 2. The microchannel module covered by a Plexi-glass shell

The fluid flows upward in the microchannel at 25°C, absorbs heat, and exits from the top. The inlet and outlet temperature of fluid and the temperature of the various points of the microchannel are measured by the thermocouples. The outlet fluid from the microchannel is introduced into the constant temperature bath to remove the heat, and then the fluid enters the collection tank at the inlet temperature. The flow rates are controlled at five values of 0.5, 1.2, 1.5, 1.8 and 2.1 l/min. A digital balance (WANT WT6002N) with the precision of 0.01 g and a stopwatch with 0.01 s sensitivity are in place to measure the mass flow rate, obtained by dividing the weight by the time span over which the sample is taken. Figure 3 shows the flow loop of the microchannel setup. The heat flux applied in this study is 56.8 kW/m².


Fig. 3. The microchannel flow loop

Data acquisitions

The amount of heat absorbed by the fluid was obtained from equation 1 where m is the mass flow rate, c_p is the heat capacity of the fluid, T_{in} is the inlet temperature and T_{out} is the outlet temperature of the fluid.

$$q_f = mc_p(T_{out} - T_{in}) \quad (1)$$

The amount of heat transferred per unit area from the surface of the microchannel to the fluid was calculated by using equation 2, where N is the number of micro-channels, L , the length of the channel, W_{ch} is the width of the channel and the H_{ch} is the height thereof.

$$q''_{conv} = \frac{q_f}{A_{conv}} = \frac{mc_p(T_{out}-T_{in})}{NL(2\eta H_{ch}+W_{ch})} \quad (2)$$

The local bulk temperature was obtained from equation 3, where η is the fin efficiency and it is near to one due to the high thermal conductivity of the microchannel alloy. Z is the axial distance from the inlet of the microchannel.

$$T_{bz} = T_{in} + \frac{q''_{conv}(2\eta H_{ch}+W_{ch})NZ}{mc_p} = \frac{Z}{L}T_{out} + \left(1 - \frac{Z}{L}\right)T_{in} \quad (3)$$

Equation 4 was used to calculate the temperature of the microchannel wall.

$$T_{wz} = T_{th} - q''_{conv} \frac{s}{ks} \quad (4)$$

Where T_{th} is the temperature indicated by the thermocouple inside the microchannel at different Z levels, S is the radial distance between the location of the thermocouples and the microchannel wall, and ks is the thermal conductivity of the microchannel modulus. The local heat transfer coefficient (h_z) was obtained from equation 5:

$$h_z = \frac{q''_{conv}}{T_{wz}-T_{bz}} \quad (5)$$

And the Reynolds number and Nusselt number were calculated as follows:

$$Re = \frac{\rho u_m D_h}{\mu} \quad (6)$$

$$Nu = \frac{h D_h}{k} \quad (7)$$

$$D_h = \frac{2w_{ch}H_{ch}}{W_{CH}+H_{ch}} \quad (8)$$

Where u_m is the fluid velocity, D_h is the hydraulic diameter, ρ and μ are the measured density and viscosity of the fluid, and h is the average heat transfer coefficient calculated numerically from the local ones. The thermal conductivity of the nanofluids, k_{nf} , is calculated as follows:

$$k_{nf} = \frac{k_p + 2k_{bf} + 2\varphi(k_p - k_{bf})}{k_p + 2k_{bf} - \varphi(k_p - k_{bf})} (k_{bf}) \quad (9)$$

The subscripts p , bf , and nf in the above relation stands for the particle (i.e. MgO), the base fluid (i.e. water) and the nanofluid, respectively.

The references of the above equations are [17, 18].

Uncertainty analysis

The uncertainty analysis was carried out using the procedure proposed by Moffat [19]. For this purpose, quantities like mass flow rate, wall temperature and fluid bulk temperature were firstly measured. Thereafter, the error of each parameter was employed in the estimation of uncertainties.

The flow rate measurement is subjected to two sources of uncertainty: the weight measurement and the time span. Since a precise digital balance was used, the uncertainty related to weighing the fluid can be neglected (± 0.01 g/2000 g). A stop watch was used to measure the time span of more than 60 s, with maximum human error of ± 0.5 s. Thus the maximum uncertainty of the mass flow rate measurement was $\pm 0.83\%$. Uncertainty of temperature measurement using K-type thermocouples was $\pm 0.1^\circ\text{C}$, and the temperature difference had an error of $\pm 0.2^\circ\text{C}$ as a result.

Considerable uncertainties in the heat transfer coefficient and thus the Nusselt number would be produced due to a small temperature difference between the microchannel surface and the fluid. The uncertainties of the measured data are shown in Table 3.

Table 3

Maximum uncertainties of the measured parameters.

Parameter	Maximum uncertainty, %
Power of heater, q_f, w	10.0
Temperature difference, $(T_{out}-T_{in}), k$	10.0
Temperature difference, $(T_w-T_b), k$	7.1
Heat transfer coefficient, $h, \text{kW/m}^2 \text{K}$	12.26
Nu	12.26
Re	0.83

RESULTS AND DISCUSSION

Figure 4 shows the variation of local heat transfer coefficients of water in different flow rates.

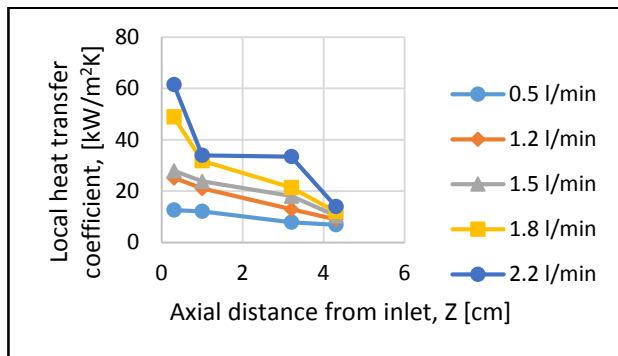


Fig. 4. The local heat transfer coefficients of water at different flow rates

According to the figure, the local heat transfer coefficient at the entrance of the microchannel has the highest value, and the closer to the end of the channel, the lower this value.

Also, with increasing flow rate (Re), the heat transfer coefficient increases. The same trend is also reported for the variation of the local heat transfer heat transfer coefficient of water in our previous experiment, shown in Figure 5.

The previous data were also obtained from a similar cylindrical microchannel, for which the hydraulic diameter is the same as that of present work, but the aspect ratios are different values [10].

One of the reasons for the increase in heat transfer coefficient at the entrance points is the thinness of thermal boundary layer at the entrance; and another reason is the formation of vortices and turbulence in the microchannel entrance region, which is intensified in higher Reynolds numbers.

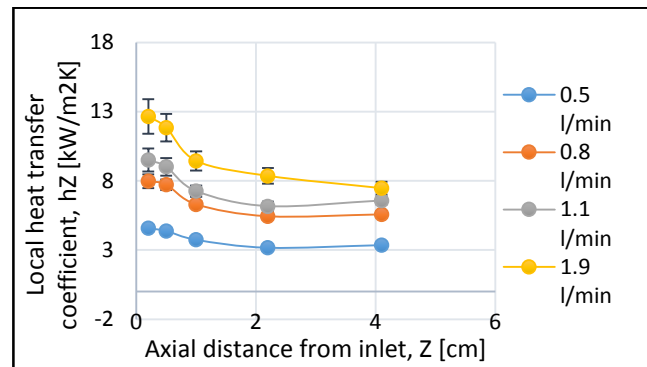


Fig. 5. Local heat transfer coefficient of water at different flow rates presented in the previous work [11]

Figure 6 shows the variation of the average Nusselt number against Reynolds number for pure water in this experiment. In this diagram, the data reported Zhang et al. [20] are also shown for comparison. Their experiments were carried out in a mini-channel with a hydraulic diameter of 1.66 mm.

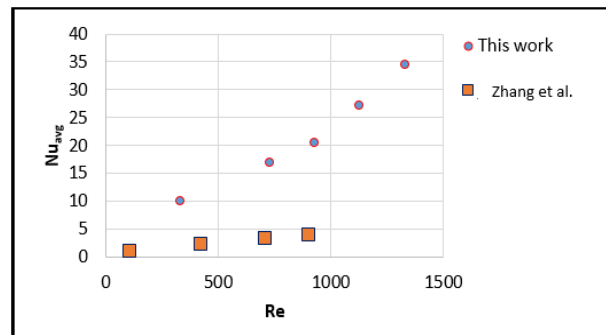
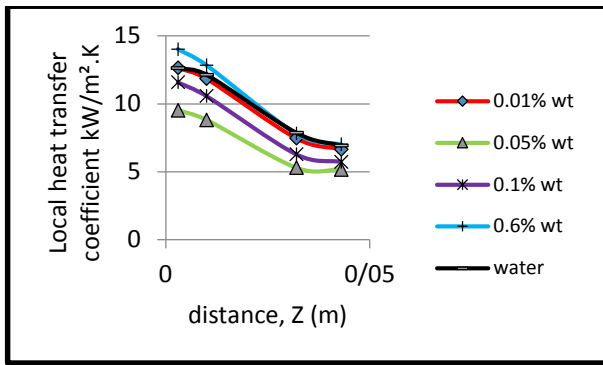


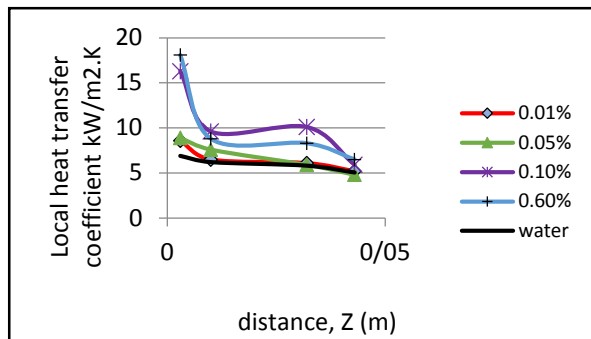
Fig. 6. Comparison between the average Nusselt in this work and the results of Zhang et al. [20]

Based on Figure 6, it turns out that the average Nusselt number in the microchannel increases with Reynolds number increase. This is also evident from the results presented by Zhang et al. [20] in minichannel, but a remarkable point in this diagram is the high amount of

Nusselt number in the microchannel compared to the mini-channel under the same conditions of the flow rate, which indicates the superiority of microfluidic devices. In order to investigate the effect of nanoparticles on local heat transfer coefficients, Figures 7(a-b) are presented at the minimum and maximum flow rates (0.5 and 2.2 l/min). According to Figure 7a, except for the concentration of 0.6 wt%, the rest of the concentrations do not generally improve the local heat transfer coefficient relative to the water, and their negative effect is observed. At the highest concentration of 0.6 wt%, the values of the local heat transfer coefficient of the nanofluid are higher than pure water. However, it is observed from Figure 7b, that all concentrations of nano magnesium oxide can make an improvement in the local heat transfer coefficient relative to water and, at the channel inlet, there is generally an increasing trend with increasing concentration. After this entrance region, it is observed that the nanofluids of 0.1 wt% is more successful than 0.6 wt% in enhancing the heat transfer coefficient. In summary, from the comparison between Figures 7(a-b) it is inferred that the enhancement of heat transfer coefficient by MgO nanoparticles depends on the flow rate, or Re. It seems that the MgO nanoparticles in accordance with their nature are more effective in a turbulent boundary layer, especially at their higher concentrations. Since the boundary layer at the entrance is more disturbed, the nanofluid of 0.6 wt% exceeded others in this region by increasing the heat transfer coefficient up to 162.3%.



(a)



(b)

Fig. 7. Local heat transfer coefficient of various concentrations of MgO nanofluid and water, (a): flow rate of 0.5 l/min, (b): flow rate of 2.2 l/min

After this region, the positive effect of 0.6 wt% nanofluids is reduced to a level which is even lower than the graph of 0.1 wt%.

As the graphs of local heat transfer coefficients of the concentrations attempted did not show a similar trend based on the applied flow rate, it is required to study the average values of heat transfer coefficient against Re, to find which concentration is more satisfactory. Figure 8 shows the average heat transfer coefficient for the concentrations of magnesium oxide/water nanofluids in this study compared to pure water.

It can be concluded that the average heat transfer coefficient of all concentrations of magnesium oxide/water is higher than that of pure water and increases with increasing Reynolds number.

The 0.6 wt% nanofluid in all Reynolds numbers studied, except $Re > 1000$, can increase the heat transfer coefficient more than other nanofluids.

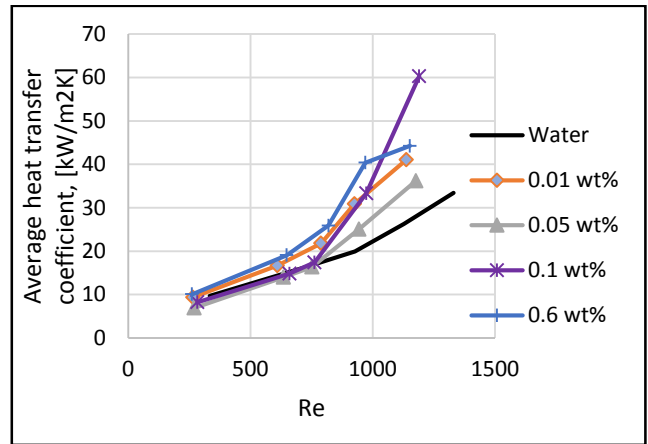


Fig. 8. Average heat transfer coefficients against Re

Figure 9 shows the Nusselt number ratio $\left(\frac{Nu(nf)}{Nu(bf)}\right)$ against Re. The ratio increases with increasing Re, and except for the 0.6 wt% nanofluid in the range of $Re > 1000$, the nanofluid can generally enhance Nusselt number relative to the base fluid in higher Re. As can be seen, a high enhancement of 52.8% in Nu is achieved by using the MgO nanofluids at 0.6wt% and at $Re=1000$.

At higher Re, increasing Nu by 0.6wt% nanofluids failed, presumably was due to the agglomeration of the nanoparticles in higher flow rates, which is previously reported at higher concentrations [10, 18, 21]. However, at the concentration of 0.1 wt%, it is observed that the ratio is monotonously increasing, with a rather sharp slope after a Re of 800, which leads to an enhancement of 80% at $Re=1200$. It can be concluded that in a more turbulent flow regime, 0.1 wt% is more effective. Other concentrations in this study, 0.01 and 0.05 wt%, did not show a significant enhancement in Nu, compared to 0.1 and 0.6 wt%.

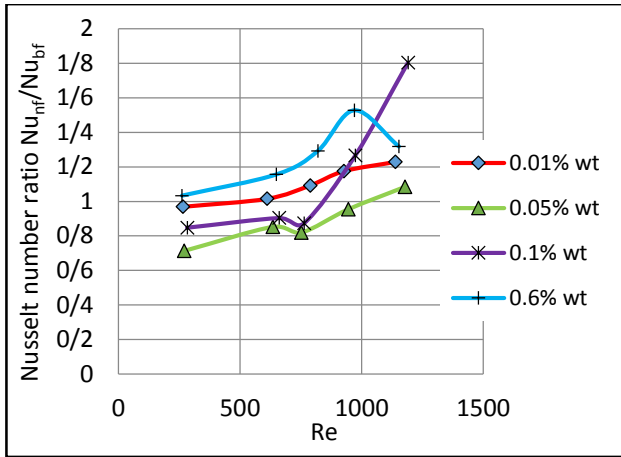


Fig. 9. Nusselt number ratios against Re

CONCLUSIONS

In this study, the thermal performance of water and nanofluid of magnesium oxide in a microchannel heat sink was investigated experimentally. The results of this research are:

A) The local heat transfer coefficients were measured and found to be large values at the channel inlet, while they decreased along the flow direction due to the variation of boundary layer thickness.

B) The local heat transfer coefficient of the nanofluids was measured at the concentrations of 0.01, 0.05, 0.1 and 0.6% by weight, and it was observed that the trend at each concentration depends on the flowrate. The heat transfer coefficient of the 0.6 wt% nanofluid at the entrance of the channel increased 162.3% relative to the water at the corresponding value.

C) Nusselt number of the MgO nanofluid increased relative to the pure water at higher Re. The 0.6 wt% was an exception, which found to decrease Nu after a Re of 1000. It was revealed that the 0.1 wt% nanofluid was more satisfactory compared to the rest of concentrations attempted, and increased the Nusselt number up to 80%.

D) It is generally concluded that the water based MgO nanofluid can enhance the heat transfer coefficient, but both of the flow rate and concentration have to be selected carefully. In a turbulent condition of the flow, lower concentrations like 0.1 wt% are more appropriate since lower amount of nanoparticles are used in the preparation process, hence are more cost effective and more easily stabilized, and on the other hand, can largely enhance the heat transfer by regulating the flow rate.

REFERENCES

[1] Tuckerman DB, Pease RF. High-performance heat sinking for VLSI. *IEEE Electron device letters*. 1981 May;2(5):126-9.

- [2] Mital M. Analytical analysis of heat transfer and pumping power of laminar nanofluid developing flow in microchannels. *Applied Thermal Engineering*. 2013 Jan 10;50(1):429-36.
- [3] Lee J, Mudawar I. Low-temperature two-phase microchannel cooling for high-heat-flux thermal management of defense electronics. *IEEE transactions on components and packaging technologies*. 2009 Jun;32(2):453-65. and *Design*. 2009 Dec 31;239(12):2992-3002.
- [4] Hassan I, Phutthavong P, Abdelgawad M. Microchannel heat sinks: an overview of the state-of-the-art. *Microscale thermophysical engineering*. 2004 Jan 1;8(3):183-205.
- [5] Mohammed HA, Bhaskaran G, Shuaib NH, Saidur R. Heat transfer and fluid flow characteristics in microchannels heat exchanger using nanofluids: a review. *Renewable and Sustainable Energy Reviews*. 2011 Apr 1;15(3):1502-12.
- [6] Esfe, M.H., Rostamian, H., Afrand, M., Karimipour, A. and Hassani, M., 2015. Modeling and estimation of thermal conductivity of MgO–water/EG (60: 40) by artificial neural network and correlation. *International Communications in Heat and Mass Transfer*, 68, pp.98-103.
- [7] Yu W, Xie H. A review on nanofluids: preparation, stability mechanisms, and applications. *Journal of nanomaterials*. 2012 Jan 1;2012:1.
- [8] Azizi Z, Alamdari A, Doroodmand M.M., Highly stable copper/carbon dot nanofluid Preparation and characterization, *Journal of Thermal Analysis and Calorimetry*. 2018 doi: 10.1007/s10973-018-7293-9.
- [9] Rimbault B, Nguyen CT, Galanis N. Experimental investigation of CuO–water nanofluid flow and heat transfer inside a microchannel heat sink. *International Journal of Thermal Sciences*. 2014 Oct 1;84:275-92.
- [10] Peyghambarzadeh SM, Hashemabadi SH, Chabi AR, Salimi M. Performance of water based CuO and Al₂O₃ nanofluids in a Cu–Be alloy heat sink with rectangular microchannels. *Energy Conversion and Management*. 2014 Oct 1;86:28-38.
- [11] Azizi Z, Alamdari A, Malayeri MR. Convective heat transfer of Cu–water nanofluid in a cylindrical microchannel heat sink. *Energy Conversion and Management*. 2015 Sep 1;101:515-24.
- [12] Azizi Z, Alamdari A, Malayeri MR. Thermal performance and friction factor of a cylindrical microchannel heat sink cooled by Cu-water nanofluid. *Applied Thermal Engineering*. 2016 Apr 25;99:970-8.
- [13] Arabpour A, Karimipour A, Toghraie D. The study of heat transfer and laminar flow of kerosene/multi-walled carbon nanotubes (MWCNTs) nanofluid in the microchannel heat sink with slip boundary

- condition. *Journal of Thermal Analysis and Calorimetry*. 2018 Feb 1;131(2):1553-66.
- [14] Barzegarian R, Aloueyan A, Yousefi T. Thermal performance augmentation using water based Al_2O_3 -gamma nanofluid in a horizontal shell and tube heat exchanger under forced circulation. *Experimental Thermal and Fluid Science*. 2016 Jun 1;74:11-8.
- [16] Jung JY, Oh HS, Kwak HY. Forced convective heat transfer of nanofluids in microchannels. *International Journal of Heat and Mass Transfer*. 2009 Jan 15;52(1-2):466-72.
- [17] Breen TJ, Walsh EJ, Punch J, Shah AJ, Bash CE. From chip to cooling tower data center modeling: Part I influence of server inlet temperature and temperature rise across cabinet. In *Thermal and Thermomechanical Phenomena in Electronic Systems (ITherm)*, 2010 12th IEEE Intersociety Conference on 2010 Jun 2 (pp. 1-10). IEEE.
- [18] Ho CJ, Chen WC. An experimental study on thermal performance of Al_2O_3 /water nanofluid in a International Communications in Heat and Mass Transfer. 2017 Aug 1;86:52-9.
- [15] Barzegarian R, Moraveji MK, Aloueyan A. Experimental investigation on heat transfer characteristics and pressure drop of BPHE (brazed plate heat exchanger) using TiO_2 -water nanofluid. minichannel heat sink. *Applied Thermal Engineering*. 2013 Jan 10;50(1):516-22.
- [19] Moffat RJ. Describing the uncertainties in experimental results. *Experimental thermal and fluid science*. 1988 Jan 1;1(1):3-17.
- [20] Zhang J, Diao Y, Zhao Y, Zhang Y. Experimental study of TiO_2 -water nanofluid flow and heat transfer characteristics in a multiport minichannel flat tube. *International Journal of Heat and Mass Transfer*. 2014 Dec 1;79:628-38.
- [21] Chein R, Chuang J. Experimental microchannel heat sink performance studies using nanofluids. *International Journal of Thermal Sciences*. 2007 Jan 1;46(1):57-66.